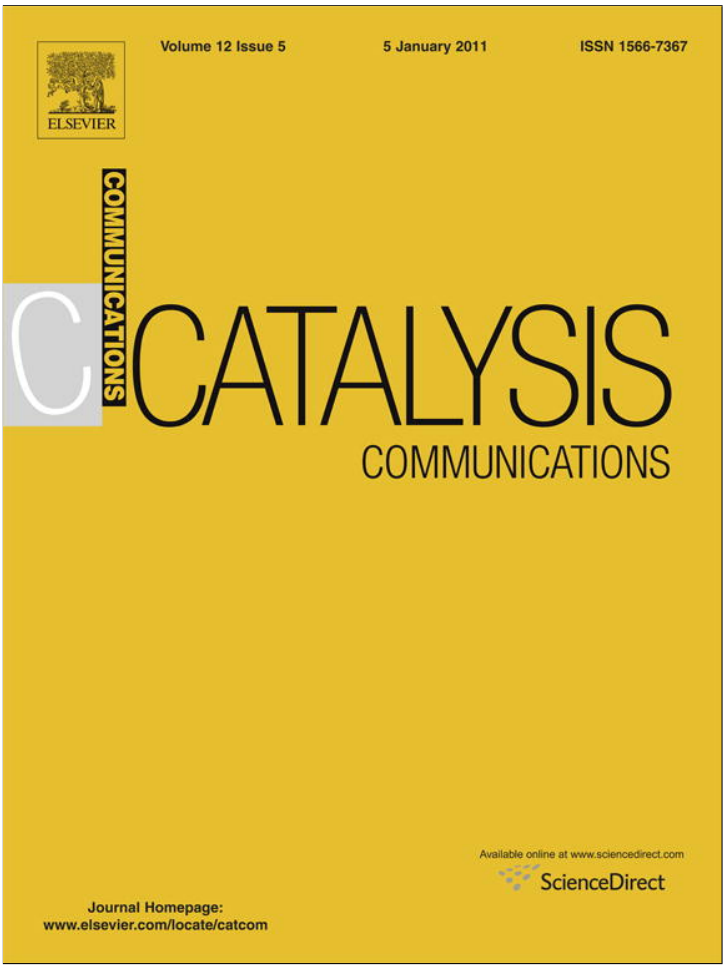

(This is a sample cover image for this issue. The actual cover is not yet available at this time.)

Catalysis Communications 17 (2012) 104–107

Contents lists available at SciVerse ScienceDirect

Catalysis Communications

journal homepage: www.elsevier.com/locate/catcom

Short Communication

Synthesis and catalytic investigation of organophilic Pd/graphite oxide nanocomposites

Á. Mastalir [a,*], T. Szabó [b], Z. Király [b], I. Dékány [b]

[a] Department of Organic Chemistry, University of Szeged, H-6720 Szeged, Dóm tér 8, Hungary
[b] Department of Physical Chemistry and Materials Science, University of Szeged, H-6720 Szeged, Aradi vt. 1, Hungary

ARTICLE INFO

Article history:
Received 28 July 2011
Received in revised form 21 October 2011
Accepted 26 October 2011
Available online 4 November 2011

Keywords:
Graphite oxide
Palladium
Nanoparticle
Alkyne hydrogenation
Turnover frequency
Selectivity

ABSTRACT

Low-loaded, organophilic Pd/graphite oxide (Pd/GO) nanocomposites were synthesized from different Pd complex precursors by applying graphite oxide as a host material and tetradecyltrimethylammonium bromide (C_{14}TAB) as a stabilizer. Structural investigation of the Pd/GO samples was performed by ICP-AES, XRD, N_2 sorption and TEM measurements. It was found that monodispersed Pd nanoparticles were formed, ranging in size between 1 and 6 nm, both on the external surface and in the interlamellar space of GO. The samples proved to be highly active and selective catalysts for liquid-phase alkyne hydrogenations. The variation in the catalytic performances was attributed to the difference in the amount of interlamellar Pd particles, which participated in the reactions as active sites.

1. Introduction

Graphite oxide (GO) is a carbonaceous layer-structured material, which may be produced by the controlled oxidation of graphite [1–4]. Since the formation of GO has been first reported [5], several preparation methods have been developed [6,7]. GO is a two-dimensional solid in bulk form, with strong covalent bonding within the layers and weaker interlayer contact between intercalated water molecules [1,3,8]. Several models have been proposed for the structure of GO [9–12]. One of the most recent models, introduced by Lerf et al. [13], describes a GO layer as a random distribution of flat aromatic regions with unoxidized benzene rings and other regions of alicyclic six-membered rings with tertiary hydroxyl and epoxide groups. The graphene oxide sheets are terminated with carboxyl groups, located only at the edges of the single GO sheets [13,14]. Unlike most lamellar compounds of graphite, GO cannot be characterized by a definite empirical formula [4], as GO is a nonstoichiometric compound and its composition depends on the synthesis conditions [3,15]. Further, GO is strongly hygroscopic and tends to decompose above 333 K [15]. GO is a hydrophilic material, which may be readily dispersed in water to form stable colloidal suspensions [1,3]. Self-assembled films can be prepared from diluted dispersions, as the GO lamellae are capable of parallel orientation [16]. As a result of liquid sorption, GO exhibits swelling and disaggregation, similarly to clay minerals [2]. GO also possesses an excellent intercalation ability and cation exchange capacity and hence a large number of intercalated GO materials have been synthesized and investigated [8,17,18]. For the preparation of metal nanoparticles on graphite oxide or graphene-derived materials, several methods have been reported in the literature [19–22], including the photochemical loading of metal nanoparticles on reduced graphene oxide sheets [21] and a special heating procedure applied for metal complexes and GO [22]. In the present study, GO has been utilized as a host material for the formation of Pd nanoparticles of controlled particle size. The structure of the Pd/GO materials has been investigated and the samples were tested as catalysts for the liquid-phase hydrogenations of terminal and internal alkynes under standard conditions. For the latter reactions, Pd has been recognized as the most selective metal [23], and Pd nanoparticles supported on layer-structured materials have been found to be particularly efficient catalysts [24,25].

2. Experimental

2.1. Preparation of Pd/GO from $Pd(NH_3)_4(NO_3)_2$

1 g of finely powdered GO was dispersed in 100 cm^3 of distilled water. After adjusting the pH to 10, the suspension was left under stirring overnight. Pd nanoparticles were generated by using the precursor $Pd(NH_3)_4(NO_3)_2$ and the cationic surfactant tetradecyl trimethylammonium bromide (C_{14}TAB). In order to ensure the complete hydrophobization of GO, an excess of C_{14}TAB was applied

* Corresponding author. Tel.: +36 62 544207; fax: +36 62 544200.
E-mail address: mastalir@chem.u-szeged.hu (Á. Mastalir).

1566-7367/$ – see front matter © 2011 Elsevier B.V. All rights reserved.
doi:10.1016/j.catcom.2011.10.028

($n_{C14TAB} = 130\ n_{Pd}$). The aqueous solution of $C_{14}TAB$ was added to the aqueous solution of the precursor and the mixture was left under stirring for 2 h. After reduction of the precursor by an excess of $NaBH_4$, the solution was added dropwise to the GO suspension. This resulted in the formation of an organophilic Pd/GO nanocomposite material. Stirring was maintained for 48 h and then the solid was centrifuged and purified by washing with a pH = 9 NaOH solution 3 times. The sample (Pd/GO1) was dried in an oven at 333 K overnight.

2.2. Preparation of Pd/GO from K_2PdCl_4

The GO suspension was prepared in the same way as mentioned above. Pd nanoparticles were obtained by using the precursor K_2PdCl_4 and the cationic surfactant $C_{14}TAB$, by applying an excess of surfactant ($n_{C14TAB} = 130\ n_{Pd}$). The precursor was dissolved in 10 cm^3 of distilled water and then the aqueous solution of the surfactant was added, resulting in the formation of a bright orange solution, which was left under stirring for 2 h. Reduction of the precursor was effected by $NaBH_4$, upon which a dark Pd sol was obtained. This was added dropwise to the GO suspension and then the mixture was left under stirring for 48 h. The sample (Pd/GO2) was purified and dried in the same way as described above. For a similar synthesis procedure, applied for Pd/hydrotalcites [25], it has been found that the effect of residual surfactant molecules on Pd was negligible and hence it was unlikely to affect the catalytic performance.

2.3. Structural characterization

The Pd contents of the samples were obtained from inductively coupled plasma atomic emission spectroscopy (ICP-AES), by using a Jobin Yvon 24 sequential ICP-AES spectrometer at 229.7 and 324.3 nm. The Pd contents for Pd/GO1 and Pd/GO2 (0.18% and 0.15%, respectively) were only slightly lower than the nominal Pd loading (0.20%).

The specific surface areas of the Pd/GO samples were determined by N_2 sorption measurements, performed by using a Micromeritics 2375 BET apparatus at 77 K.

X-ray diffraction (XRD) measurements were performed with a Philips PW 1820 diffractometer (40 kV, 35 mA, CuK_α radiation). The basal spacings of the samples were determined from the first-order Bragg reflections, by applying a PW 1877 software.

TEM measurements were effected by using a Philips CM10 transmission electron microscope, equipped with a LaB_6 cathode and a Megaview II digital camera. The particle size distributions and the mean particle diameters were determined as $\Sigma n_i d_i / \Sigma n_i$ ($\Sigma n_i > 250$), by using AnalySIS 3.1. software. The dispersions of the catalysts were calculated from the mean particle diameters d, as $D = 0.885/d$ [26].

2.4. Catalytic test reaction

The Pd/GO materials were tested as catalysts in an automated hydrogenation apparatus [25], for the liquid-phase hydrogenations of 1-pentyne, 1-hexyne, 3-hexyne, 1-heptyne and 1-phenyl-1-butyne. For each measurement, 5 mg of sample was used. The reactions were investigated at 298 K and 10^5 Pa, with a reactant:Pd (R:Pd) ratio of 2500. Pretreatment of the catalyst was carried out in static hydrogen at 298 K for 60 min, followed by the addition of solvent (1 cm^3 of toluene), and stirring for 45 min. All reactions were performed under vigorous stirring (1400 rpm) to eliminate mass transport limitations. The hydrogen consumption was recorded as a function of reaction time. The reaction rates were determined from the slopes and the turnover frequencies (TOF) were calculated as $TOF = 7.2538 \cdot 10^{-5}\ RS/D$ [s^{-1}], where RS is the initial rate and D is the dispersion of the catalyst. Quantitative analysis of the products was performed with an HP 5890 gas chromatograph equipped with a HP-I capillary column and a flame ionization detector (FID). The experimental error was ±2% for repeated runs.

3. Results and discussion

The specific surface areas of the Pd/GO samples were very low (2.5 $m^2\ g^{-1}$ and 3.5 $m^2\ g^{-1}$ for Pd/GO1 and Pd/GO2, respectively), indicating that the interlayers of organophilic GO were highly loaded with alkyl chains, as related to the intercalation of $C_{14}TAB$ molecules, and therefore N_2 adsorption took place on the external surfaces of the GO particles.

The pore size distribution could not be determined, as GO was found to be a nonporous material.

The XRD patterns of GO and the Pd/GO nanocomposites are demonstrated in Fig. 1. For the GO host, a well-defined peak was obtained at $2\Theta = 12.9°$, which corresponds to an interplanar distance (d_L) of 0.69 nm. The characteristic d_{002} reflection of graphite at 26.6° could not be observed, which confirmed that complete oxidation took place [27]. As a result, a well-ordered, lamellar structure was formed, which was more open than that of graphite ($d_L = 0.336$ nm) and thus more susceptible to intercalation [27]. The pattern of Pd/GO1 is comprised of three peaks at $2\Theta = 7.82$, 9.08, and 18.16°. The latter peaks characterize the same basal spacing, 0.97 nm. The first reflection, appearing with smaller intensity, belongs to another phase, in which the c-axis repeat distance is 1.13 nm. These distances indicate that both phases comprise of surfactant-stuffed interlayers with slightly different amounts or conformations of the intercalated molecules. Pd/GO2 shows a similar diffractogram, but the first two reflections are markedly shifted toward lower diffraction angles (with d-values of 1.4 and 1.2 nm). On the other hand, the position of the $2\Theta = 18°$ ($d = 0.5$ nm) peak remained unchanged. Since the related distance is too low to be accounted for a first-order reflection of GO ($d_{001} = 0.66$ nm for the air-dry sample, whereas the lowest values for anhydrous Brodie-GOs are ca. 0.59 nm [15]), we still assign this peak as a second-order reflection. The fact that the peaks no longer occur at integral d-values suggests that randomly interstratified structures were formed, that is, the structure, conformation and interlayer concentration of surfactant molecules were different. Nevertheless, the relatively low interlamellar distance implies that the density of accommodated surfactant molecules is not too high and the molecules lie flat and take a monolayer arrangement [17]. The XRD patterns do not give conclusive evidence whether the Pd nanocrystals are inserted between the GO layers, because the Pd loadings are lower than the detection limit for ultrafine crystallites generally exhibiting significant broadening and concomitant intensity loss, to which interstratification may also contribute.

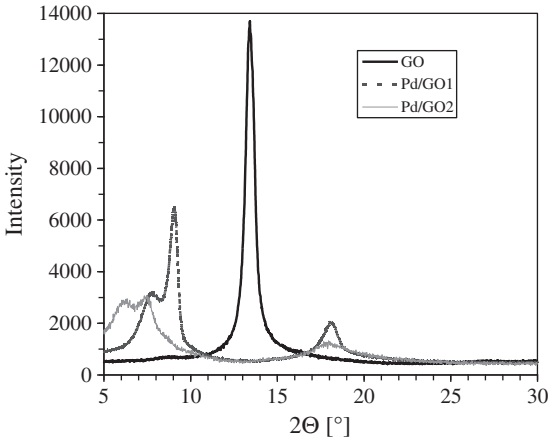

Fig. 1. XRD patterns of GO, Pd/GO1 and Pd/GO2.

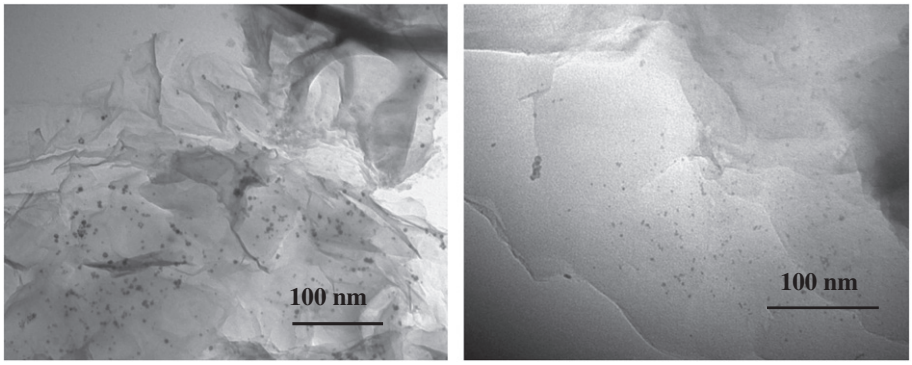

Fig. 2. TEM images of the Pd/GO nanocomposites.

Figs. 2 and 3 display the TEM images and the particle size distributions of the Pd/GO samples, respectively. The formation of the Pd nanoparticles had no effect on the lamellar structure of the GO host material. A large number of quasi-spherical surface Pd particles can be distinguished, for which aggregation did not occur. For Pd/GO1, the particle diameters fell in the range 1–6 nm. The highest relative frequencies were observed for the 2–4 nm Pd particles (77%), whereas the number of Pd particles smaller than 2 nm and larger than 4 nm was negligible. This finding confirms the steric stabilizing effect of the cationic surfactant molecules, which prevented particle aggregation [24,25]. The mean particle diameter of the Pd particles was 3.6 nm and the dispersion of the sample was 25%. The Pd particles for Pd/GO2 proved to be small, quasi-spherical and monodispersed, similarly as those for Pd/GO1. The majority of the particles (86%) fell in the range 1–3 nm. The mean particle diameter was 2.5 nm and the dispersion was 36%. The application of different precursors may result in the formation of different species, which may affect the reduction procedure. Previous studies for $K_2[PdCl_4]$ indicated that the application of a large excess of C_{14}TAB resulted in a ligand exchange reaction with free Br^- [28,29], resulting in the formation of $(C_{14}TA)_2[PdBr_4]$, attached to free C_{14}TAB micelles. On the other hand, for the precursor $Pd(NH_3)_4(NO_3)_2$, an electrostatic interaction with Br^- anions and a ligand exchange reaction of NH_3 with the $C_{14}TA^+$ may be suggested. As reported for positively charged Pd(II) complexes bound to anionic surfactant micelles, both electrostatic and hydrophobic interactions are to be considered in the binding process [30].

The catalytic performances of the Pd/GO nanocomposites were investigated in liquid-phase alkyne hydrogenations, typically regarded as zero-order reactions, for which the reaction rate is independent of the reactant concentration [31,32].

This implies that the initial rate remains constant until all the reactant has been transformed. The results obtained for the hydrogenations of terminal and internal alkynes over Pd/GO1 are summarized in Table 1. It may be observed that Pd/GO1 was a highly active catalyst for alkyne hydrogenations. For the transformations of terminal alkynes, the reaction rates and the turnover frequencies displayed no systematic variation with the reactant size. The highest reaction rate was obtained for 3-hexyne. On the other hand, the reaction rate for the hydrogenation of 1-phenyl-1-butyne was considerably lower, and decreased with the reaction time. This finding may be regarded as an indirect evidence for the formation of interlamellar Pd crystallites in the GO host [25], as the latter crystallites could not be identified by XRD. Such interlamellar clusters may also be regarded as active sites and tend to be less accessible for 1-phenyl-1-butyne, comprising an aromatic ring and an internal alkyne group [19,20]. The selectivity toward the formation of the main products alkene and *cis*-alkene exceeded 90% for each reactant and was nearly 100% for the reactions of 1-pentyne and 3-hexyne. This implies that overhydrogenation and the formation of by-products (either 2-alkene or *trans*-alkene) were negligible. It may therefore be established that Pd/GO1 was a particularly efficient catalyst for the hydrogenations of aliphatic alkynes, for which high conversions and alkene selectivities were achieved at short reaction times.

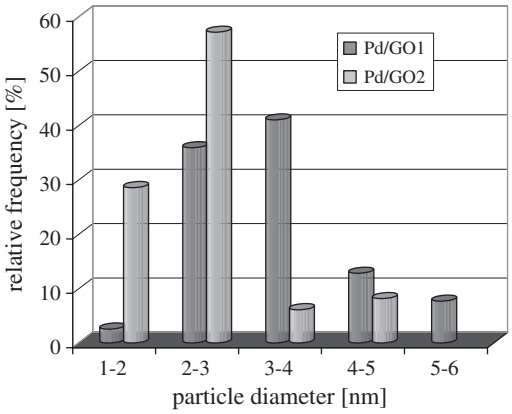

Fig. 3. Particle size distributions of the Pd/GO nanocomposites.

The data obtained for the catalytic investigation of Pd/GO2 for the same reactions are displayed in Table 2. Although the Pd contents of the Pd/GO nanocomposites were very similar, the initial rates and the TOF values for Pd/GO2 were considerably lower than those for Pd/GO1. This suggested limited access for the reactant molecules to the active centers in the interlamellar space of GO. The highest conversions were obtained for the hydrogenations of lower alkynes, whereas Pd/GO2 proved to be a less efficient catalyst for the reactions of 1-heptyne and 1-phenyl-1-butyne. The catalytic performance of Pd/GO2 decreased with increase of the reactant size. It may therefore be suggested that a significant proportion of the catalytically active Pd nanoparticles was situated in the interlamellar space of GO and the latter particles were less accessible for the reactants than those on the external surface of the GO host. The selectivities for the formation of the main products were similar to those obtained for Pd/GO1. Overhydrogenation was insignificant for each reactant. For the hydrogenations of terminal alkynes, small amounts of 2-alkenes were detected as by-products, formed by isomerization [23]. The results

Table 1
Hydrogenations of alkynes over Pd/GO1.

Reactant	Time [min]	R [$cm^3\ min^{-1}\ g^{-1}$][a]	TOF [s^{-1}]	Conversion [%]	S [%][b]
1-pentyne	21	24,475	7.1	97.0	99.5
1-hexyne	33	17,529	5.1	97.6	97.6
3-hexyne	43	31,407	9.1	91.1	99.9
1-heptyne	21	26,726	7.8	96.6	90.6
1-phenyl-1-butyne	69	3287	1.0	27.8	94.6

[a] Reaction rate.
[b] Selectivity of the main reaction product (1-alkene and *cis*-alkene for terminal and internal alkynes, respectively).

Table 2
Hydrogenations of alkynes over Pd/GO2.

Reactant[a]	R [$cm^3\ min^{-1}\ g^{-1}$][b]	TOF [s^{-1}]	Conversion [%]	S [%][c]
1-pentyne	13,653	2.8	78.6	98.2
1-hexyne	14,034	2.8	88.1	95.1
3-hexyne	8310	1.7	63.5	98.3
1-heptyne	6148	1.2	14.7	100
1-phenyl-1-butyne	1045	0.2	6.4	100

[a] t = 45 min.
[b] Reaction rate.
[c] Selectivity of the main product (1-alkene or *cis*-alkene).

of the catalytic test reactions confirmed that Pd/GO1, obtained from the precursor $Pd(NH_3)_4(NO_3)_2$, was a more efficient catalyst than Pd/GO2, prepared from K_2PdCl_4. As the structures of the Pd/GO nanocomposites and the size distributions of their surface Pd particles were very similar, the difference in their catalytic performance may be related to their interlamellar Pd content. The evidence that the particle diameters for Pd/GO2 were smaller than those for Pd/GO1 (Fig. 3) indicated that Pd/GO2 was more likely to accommodate an enhanced amount of interlamellar Pd particles. It may be established that both the surface and interlamellar Pd particles participated in the reactions as active sites. The catalytic behavior of Pd/GO1 was basically determined by its Pd content located on the external surface of GO, and hence this sample may be regarded as a GO-supported Pd catalyst. On the other hand, an enhanced amount of interlamellar Pd nanocrystals, as suggested for Pd/GO2, tends to decrease the catalytic performance. For the transformation of 3-hexyne, the Pd/GO samples proved to be more efficient than the conventional supported Pd catalysts [20], as the former samples provided better alkene selectivities at high conversions.

4. Conclusions

Graphite oxide was utilized as a host material for the generation of Pd nanoparticles with controlled particle size. Low-loaded, organophilic Pd/GO nanocomposites were prepared by using different complex precursors and C_{14}TAB as a stabilizer. Structural investigation confirmed that an efficient particle size control was achieved and the formation of Pd nanoparticles had no effect on the structure of the GO host. It was found that Pd nanoparticles were formed both on the external surface and in the interlamellar space of GO. The Pd/GO samples were tested as catalysts in the liquid-phase hydrogenations of terminal and internal alkynes. Both samples proved to be efficient catalysts for the reactions of lower alkynes. As compared with Pd/GO1, Pd/GO2 was suggested to comprise an enhanced amount of interlamellar Pd particles, which were less accessible for reactants than those on the external surface of GO. Pd/GO1 proved to be a particularly efficient catalyst, which provided high conversions and alkene selectivities at short reaction times.

Acknowledgment

Financial support provided by the TÁMOP-4.2.1/B-09/1/KONV-2010-0005 project is gratefully acknowledged.

References

[1] S. Stankovich, R.D. Piner, S.T. Nguyen, R.S. Ruoff, Carbon 44 (2006) 3342–3347.
[2] I. Dékány, R. Krüger-Grasser, A. Weiss, Colloid & Polymer Science 276 (1998) 570–576.
[3] T. Szabó, E. Tombácz, E. Illés, I. Dékány, Carbon 44 (2006) 537–545.
[4] R.J. Beckett, R.C. Croft, The Journal of Physical Chemistry 56 (1952) 929–934.
[5] B. Brodie, Annals Chimie Physical 59 (1860) 466–472.
[6] L. Staudenmaier, Berichte der Deutschen Chemischen Gesellschaft 31 (1898) 1481–1487.
[7] W.S. Hummers, R.E. Offemann, Journal of the American Chemical Society 80 (1958) 1339-1339.
[8] Z. Liu, Z.M. Wang, X. Yang, K. Ooi, Langmuir 18 (2002) 4926–4932.
[9] A. Clauss, R. Plass, H.P. Boehm, U. Hofmann, Zeitschrift fur Anorganische und Allgemeine Chemie 291 (1957) 205–220.
[10] G. Ruess, Monatshefte fur Chemie 76 (1946) 381–417.
[11] M. Mermoux, Y. Chabre, A. Rousseau, Carbon 29 (1991) 469–474.
[12] T. Nakajima, Y. Matsuo, Carbon 32 (1994) 469–475.
[13] H. He, T. Riedl, A. Lerf, J. Klinowski, The Journal of Physical Chemistry 100 (1996) 19954–19958.
[14] S. Stankovich, R.D. Piner, X. Chen, N. Wu, S.T. Nguyen, R.S. Ruoff, Journal of Materials Chemistry 16 (2006) 155–158.
[15] T. Szabó, O. Berkesi, P. Forgó, K. Josepovits, Y. Sanakis, D. Petridis, I. Dékány, Chemistry of Materials 18 (2006) 2740–2749.
[16] N.A. Kotov, I. Dékány, J.H. Fendler, The Journal of Physical Chemistry 99 (1996) 13065–13069.
[17] Y. Matsuo, T. Niwa, Y. Sugie, Carbon 37 (1999) 897–901.
[18] Y. Matsuo, T. Miyabe, T. Fukutsuka, Y. Sugie, Carbon 45 (2007) 1005–1012.
[19] Á. Mastalir, Z. Király, M. Benkő, I. Dékány, Catalysis Letters 124 (2008) 34–38.
[20] Á. Mastalir, Z. Király, Á. Patzkó, I. Dékány, P. L'Argentiere, Carbon 46 (2008) 1631–1637.
[21] G. Moon, Y. Park, W. Kim, W. Choi, Carbon 49 (2011) 3454–3462.
[22] K. Gotoh, T. Kinumoto, E. Fujii, A. Yamamoto, H. Hashimoto, T. Ohkubo, A. Itadani, Y. Kuroda, H. Ishida, Carbon 49 (2011) 1118–1125.
[23] Á. Molnár, A. Sárkány, M. Varga, Journal of Molecular Catalysis A: Chemical 173 (2001) 185–221.
[24] Á. Mastalir, Z. Király, Gy Szöllősi, M. Bartók, Journal of Catalysis 194 (2000) 146–152.
[25] Á. Mastalir, Z. Király, Journal of Catalysis 220 (2003) 372–381.
[26] P.C. Aben, Journal of Catalysis 10 (1968) 224–229.
[27] C. Hontoria-Lucas, A.J. López-Peinado, J. de López-González, M.L. Rojas-Cervantes, R.M. Martín-Aranda, Carbon 33 (1995) 1585–1592.
[28] B. Veisz, Z. Király, L. Tóth, B. Pécz, Chemistry of Materials 14 (2002) 2882–2888.
[29] L. Bisson, C. Boissiere, L. Nicole, D. Grosso, J.P. Jolivet, C. Thomazeau, D. Uzio, G. Berhault, C. Sanchez, Chemistry of Materials 21 (2009) 2668–2678.
[30] F.P. Cavasino, C. Sbriziolo, M. Cusumano, A. Gianetto, Journal of the Chemical Society, Faraday Transactions 92 (1996) 2263–2268.
[31] G. Carturan, G. Facchin, G. Cocco, S. Enzo, G. Navazio, Journal of Catalysis 76 (1982) 405–417.
[32] C.A. Hamilton, S.D. Jackson, G.J. Kelly, R. Spence, D. de Bruin, Applied Catalysis A: General 237 (2002) 201–209.